Tissue characterisation by ultrasound strain imaging

Methodological aspects and gastroenterological applications

Roald Flesland Havre

Dissertation for the degree philosophiae doctor (PhD)

at the University of Bergen

2012

Dissertation date: October 11th, 2012

”Measure what is measurable, and make measurable what is not”

Galileo Galilei (1564-1642)

Scientific environment

Institute of Medicine, Section for Gastroenterology,
Faculty of Medicine and Dentistry,
University of Bergen, Norway

National Centre for Ultrasound in Gastroenterology,
Division of Gastroenterology, Department of Medicine,
Haukeland University Hospital, Bergen, Norway

Medviz – An interdisciplinary initiative to promote Research & Development in medical imaging and advanced visualisation at Haukeland University Hospital, University of Bergen and Christian Michelsen Research (CMR)

Table of contents

Acknowledgements

This work was carried out at the University of Bergen, Institute of Medicine, Section for Gastroenterology from March 2008 to March 2012. The "prologue" had then been financed by the National Centre for Ultrasound in Gastroenterology (NCUG) at Haukeland University Hospital. In 2006 we started to plan this work and to collect and analyse data on the first in-vitro study resulting in the first paper in this thesis. During the course of collecting data for the publications in this thesis, I was introduced to the world of endoscopic ultrasonography (EUS). **Lars Birger Nesje** has been my principal supervisor in the scientific work, besides holding the position as Director of the Department of Medicine. I am very thankful for the time you have spent, your good moods, your thoughtful remarks and improvements to my manuscripts and your ability to make me more optimistic whenever I left your office than when I came in. Professor and former director of NCGU **Svein Ødegaard** has left me the legacy and responsibility of endoscopic ultrasonography. You have always been supportive and with great expectations for our work. You have given me insight to the history of ultrasound in gastroenterology and we have had many good discussions over several issues. My second co-supervisor is Professor **Odd Helge Gilja**. You played an important role for recruiting me into ultrasound research, and opening my eyes to an ultrasound perspective. You have inspired me and given me important advice on the way. You are visionary and have succeeded in establishing the Medviz research cluster in medical imaging. You have introduced me to the national and international ultrasound community and I have also enjoyed your company on journeys to several ultrasound conferences.

Of my co-workers at the NCUG, **Eva Fosse** has contributed a lot to the completion of the research projects. Her friendliness and practical experience with ultrasound equipment such as EUS scopes, FNA needles and patient comfort is exquisite. Also co-workers at the Medical Department have supported the projects and I want to thank **Vibecke Lindøen**, the leader of our endoscopy unit for being positive and compliant with research activities despite limited time and personnel resources. Also

Geir Folvik, former head of the gastroenterology section in the Medical Department has always been supportive of my projects.

My gratitude goes to persons who contributed substantially in some way, and who many are co-authors of the papers: Professor **Knut Matre**, Institute of Medicine (ultrasound), Professor **Geir Egil Eide**, (statistics), Pathologist **Sabine Leh**, (data collection, preparation and pathological examinations). **Erlend Elde**, who wrote a student essay on sonoelastography and contributed to the data collection in the first paper, Professor **Gunnar Baatrup**, Department of Surgery, Dr. **Dag Hoem**, Department of Surgery, HUS and the personnel at the Surgical Operation Unit (SOP) who let me come to collect specimens, and sometimes scan patients during the surgical procedures. **Dag Magne Ulvang**, CMR helped set up a haptic image device. I am grateful to professor **Adrian Saftoiu** from Craiova, Romania who invited us to contribute to the European EUS Elastography Multicentre Study on pancreatic lesions. I want to thank representatives from Hitachi Medical Corporation, Europe, **E. Bibby** and application specialist Dr. **K. Kukulski** for providing invaluable insights to the scanner's elastography algorithm.

To my fellow researchers: **Jo Waage** for taking the chance and becoming a partner in endoscopic ultrasonography and elastography and mutually increase each other's insight to methodology and the clinical applications. To **Kim Nylund**, **Vernesa Dizdar**, **Kurt Hanevik**, **Rune Nilsen**, **Kristine Lillestøl** for sharing knowledge and advice in the same office with me and **Aymen B. Ahmed**, **Dag Arne Lihaug Hoff**, **Maja Mujic** and **JørgenValeur** thank you for your company, your comfort, advice and support through the recent years. I also want to thank **the patients** who gave their consent to participate in the studies. Last but not least, I will thank my wife, **Katrine.** Your love and support has been pivotal for the completion of this thesis. You have patiently awaited the completion of my PhD work and have provided for our family of six. I also want to thank our four children **Håkon, Eirik, Ingrid** and **Sigurd** for motivation and reminding me about great tings in life.

List of papers

Paper 1: Havre RF, Elde E, Gilja OH, Ødegaard S, Eide GE, Matre K, Nesje LB. *Freehand Real-Time Elastography: Impact of Scanning Parameters on Image Quality and in Vitro Intra- and Interobserver Validations.* Ultrasound Med Biol 2008;34:1638-1650

Paper 2: Havre RF, Waage JR, Gilja OH, Odegaard S, Nesje LB. Real-Time Elastography: *Strain Ratio Measurements Are Influenced by the Position of the Reference Area.* Ultraschall in Med 2011. E-pub ahead of print, June 15. 2011

Paper 3: Havre RF, Leh S, Gilja OH, Ødegaard S, Waage JER, Baatrup G, Nesje LB. *Strain Assessment in Surgically Resected Inflammatory and Neoplastic Bowel Lesions.* Ultraschall in Med, Accepted in final version Sept. 15th 2012.

Paper 4: Havre RF, Ødegaard S, Gilja OH, Nesje LB: *Characterisation of Focal Pancreatic Lesions using Endoscopic Ultrasonography with Real-Time Elastography.* Submitted June 2012.

Abbreviations

ARFI – Acoustic Radiation Force Impulse

EC – Elastic Contrast

ECAM – Extended Combined Autocorrelation Method

EUS – Endoscopic Ultrasonography

ROI – Region of Interest

RTE – Real Time Elastography

SWI – Shear Wave Imaging

SR – Strain Ratio

SRI – Strain Rate Imaging

SSI – Supersonic Shear Imaging

TE –Transient Elastography

TM – Tissue mimicking

US – Ultrasonography

VA – Vibro Acoustography

VAS – Visual Analogue Scale

VCS – Visual Categorical Score

VE – Vibro Elastography

Abstract

Real-Time Elastography (RTE) is a new imaging modality that monitors tissue strain during applied stress. The aim of this thesis was to validate if RTE was a reliable modality to reflect pathologically induced differences in elasticity or tissue hardness and to interrogate if assessment of elastic changes by RTE could be used as a diagnostic tool in clinical practice. Particularly, we focused on the ability of RTE to differentiate between benign and malignant disease in intestinal and pancreatic lesions.

Two validation studies were performed using a tissue-mimicking phantom containing inclusions with different size, depth and defined elastic properties. We evaluated the influence of different parameter settings on image quality, and intra- and interobserver variation was also assessed. Furthermore, we examined the impact of different size and depth of selected calculation areas in strain ratio (SR) measurements. In a sub-study on resected bowel specimens, elastograms were compared with histology in order to verify the ability to differentiate between benign and malignant disease and study mechanisms leading to changes in elastic properties. In a clinical study on focal pancreatic lesions, RTE was performed using endoscopic ultrasonography (EUS). In the evaluation of strain images from human tissue we applied a previously published visual categorical score (VCS), a visual analogue scale (VAS) and SR.

The validation studies confirmed RTE's ability to assess elastic properties in vitro with fair to good inter- and intraobsever agreement. The level of dynamic range influenced image quality but had no impact on SR measurements. On the other hand, we found that the reference areas' distance from the US transducer but not the size influenced significantly on SR measurements. In resected bowel lesions, no significant strain difference was found between stenotic lesions caused by Crohn's disease and adenocarcinomas. EUS-based RTE of pancreatic lesions showed significant strain difference between the entities of benign and malignant lesions, but the variation within the entities was substantial.

1. Introduction

1.1 Background

The distinction between malignant and benign disease from medical images represents a major challenge to clinicians and radiologists every day. The description of hard tissue as a sign of serious illness is described in early historical sources such as Ebers papyrus (1552 BC) [1,2], and palpation of organs remains an important clinical examination tool to date.

The prospect of using new methods and technology in order to improve distinction between malignant tumours and benign lesions is alluring. If this would be possible, tumours could be discovered at less advanced stages. Earlier and more accurate diagnostics could lead to improved and more efficient treatment. A better diagnostic may also lead to avoidance of futile surgery in patients with advanced disease or lesions of benign entity.

Increased tissue stiffness is a common feature of many cancers through a process called desmoplasia where tumour tissue becomes increasingly fibrotic due to up-regulation of growth factors or their receptors. Furthermore, increased interstitial pressure is a typical feature of many malignant tumours. Imaging local differences in tissue strain may provide new diagnostic information, which may enhance tissue characterisation, and possibly improve distinction between benign and malignant lesions, and this possibility has been a main motivation for this PhD-thesis.

1.2 Principles of ultrasound (US) imaging

Ultrasound is the term used for sound waves with frequency ranging from 20kHz to more than 200MHz, thus above the audible range for humans. Ultrasound waves are longitudinal waves, which means they create transient compressions of the media they are travelling through [3]. Ultrasound has been applied for medical imaging since more than 50 years. A sound source, typically made of a piezo-electrical

material, emits an US wave and records the reflected US signal. Several elements can be combined in an US probe in various patterns (linear, curved, annular). The physical imaging is based on reflection of the sound waves from structure variation within the body. Reflection takes place when the sound waves cross into a tissue structure with different acoustic impedance, a product of the speed of sound and tissue density.

A fraction of the sound energy is reflected to the ultrasound probe. The reflected signals can be temporally and spatially combined to constitute an acoustic representation of the anatomy. US is generally cheaper and more mobile than alternative imaging techniques such as CT or MRI. It is also considered as a safe imaging modality, since it does not produce ionizing radiation. However, the safety aspects are constantly under surveillance by international ultrasound societies [4]. Safety, spatial resolution and excellent ability to travel in fluids, has given US a leading role in obstetric imaging. In cardiology the good temporal resolution and Doppler imaging has established echocardiography as a principal imaging modality for cardiac function. Currently, ultrasound is a widely used imaging modality in several fields of medicine. As far as abdominal ultrasonography is concerned, the study of the liver, pancreas, spleen, kidneys, vessels, stomach and intestines are among the established clinical applications.

Propagation of US waves

Longitudinal (compressional) waves, such as US waves, are dependent on the tissue density, ρ and the bulk modulus, K [5]. The propagation speed for longitudinal waves in biological tissue can be expressed as:

$$c_L = \frac{K}{\rho}$$

The formula for bulk modulus, K is thus: $K = c_L \rho$

Propagation speed in soft tissue has a limited range, from 1470 m/s in fat to 1620 m/s in muscle tissue [6], commonly approximated to 1540 m/s for practical purposes in

US scanners. Also, the range of soft tissue's densities is limited. Consequently, the bulk modulus *K* has a limited dynamic range.

1.3 Principles of elasticity and strain imaging

Imaging of soft tissue elasticity started by recording the correlation coefficients of consecutive US A-scans of liver tissue in response to arterial pulsations [7,8]. One of the first papers describing ultrasonic evaluation of physical properties including compressibility, was published on breast tumours in-vivo by Ueno et al. in 1988 [9]. Following the introduction of Doppler techniques, several applications for tissue-Doppler were proposed for diagnostic purposes including vascular wall stiffness and myocardium. A pulsed Doppler system was proposed for measuring the mechanical properties in soft tissue, and the method was compared to a mechanical testing in contracting muscle in 1987 [10]. In 1991, Ophir and co-workers published the first comprehensive method description using the term "elastogram" to describe a qualitative strain map emerging from quasi-static compression [11], Subsequently, the term has been applied for qualitative strain maps based on various algorithms. The same research group have published substantial literature online [12]. A review of their pioneer work was published in 2002 [5]. Feasibility of free-hand application of US-based strain imaging was performed in the evaluation of breast tumours in 1988 [9]. Subsequently, after the introduction of free-hand strain imaging modalities in commercial scanners, a majority of clinical applications are based on free-hand techniques. Recent comprehensive reviews on US strain and elasticity imaging methods and their current documentation and applications are published by Parker et al. 2011[13] and Wells and Lang 2011[2].

1.3.1 Definitions

Stress (σ) may be described as a vector with size and direction.

Strain (*ε*) is defined by the formula: $$\varepsilon = \frac{(L1 - L2)}{L1} = \frac{\Delta L}{L1}$$

where L1 is initial length, L2 is length after compression/stretching. Strain has no unit, but is frequently measured in percent (%). It is a result of stress on a viscoelastic or elastic material [14].

Elasticity (E) is defined as stress/strain $E = \frac{\sigma}{\varepsilon}$ measured with the unit kPa.

Elastic modulus (Young's modulus) is expressed as the slope of the stress-strain curve.

Strain attenuation describes the reduction of strain as the stress is absorbed when it moves through a viscoelastic medium.

Viscoelastic: Used to describe the dual nature of biological soft tissue having both elastic and viscous properties.

Hooke's law: $F = -kx$

F=force, equivalent to stress (σ). *–k*: spring constant, *x*: displacement (equivalent to strain, ε). Describes a linear elasticity system, such as homogeneous, isotropic materials.

Isotropic material: a material that has the same strain response for all directions of tissue stress.

Free-hand elastography: Strain image created on the basis of autocorrelation of echo-positions in a B-mode ultrasound image without knowledge of the amount of stress applied or the pre-compression of the medium. Assumes equal stress application over the region of interest.

Real-time elastography: Extended Combined Autocorrelation Elastography used in Hitachi scanners used for the work in this thesis. Provides a qualitative strain map simultaneous with the B-mode presentation. Is designed for free-hand applications.

1.3.2 Relationship between stress, strain and elasticity

Elasticity, *E* is defined as strain divided by stress (σ/ε). For materials with linear elasticity (e.g. gelatine) the E is the same at all levels of stress (linear curve). For most biological tissues, strain increases with the amount of stress (non linear strain). Autocorrelation strain imaging algorithms are generally based on Hooke's law (F=-kx). For a limited stress/strain interval, the curve may be regarded as linear and according to Hooke's law even in biological tissue. Another assumption that has to be met to make such calculations eligible is that the tissue can be regarded as homogeneous and isotropic.

Stress/Strain curve in gelatine and in biological tissues:

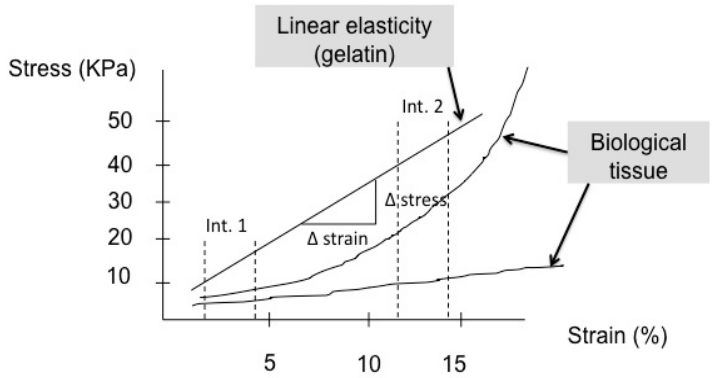

Figure 1: Stress/Strain curve. The autocorrelation software assumes linearity within the interval of straining (Int.1 or Int. 2). The illustration shows how the elasticity changes in biological tissues when different levels of pre-compression is applied prior to a cyclic stress within two separate intervals for the same tissue. The difference in strain between tissue A and B is larger in interval 2 than in interval 1. In strain imaging, the stress amount is not registered, however for RTE, strains in the range of 0.1-2 % provides best images. (Based on T.Krouskop, 1998) [15]

1.4 Ultrasound methods for elasticity and strain imaging

1.4.1 Autocorrelation (Quasi-static Elastography)

The method combines B-mode ultrasonography with recorded strain caused by external stress. An applied force can generate such stress when the examiner is moving the probe repetitively or internally, as in endoscopic elastography, by respiratory movements or cardiovascular pulsations. Most commercial US scanners that offer an elastography mode on their scanners apply an algorithm of autocorrelation of US RF-signals or tissue Doppler.

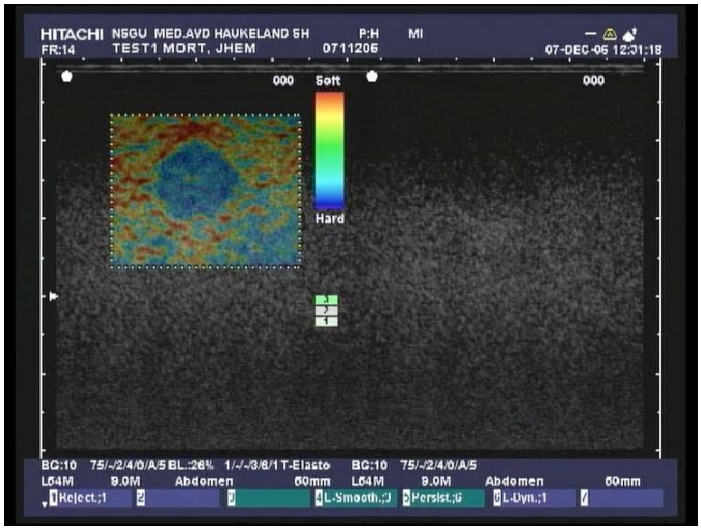

Figure 2: Free-hand RTE strain imaging of spherical inclusion in a TM-phantom (CIRS Model 49). In the B-mode image (right), the inclusion is hardly visible. The inclusion is harder than the surrounding material (58 KPa vs. 30 kPa). The Elasticity dynamic range (E-dyn) is set to the lowest level (1) allowing visualisation of small elastic contrasts. Blue colour indicates harder tissue (low strain), while red/yellow indicate softer tissue.

At this E-dyn setting, very little green colour is displayed, due to the dichotomous elastic moduli present in the phantom. The stress source is placed above the lesion (exerted by the transducer). Increased strain is visualised directly above the harder lesion indicating the direction of the stress. Despite homogeneous and isotropic qualities, strain variation is observed in the surrounding material, indicating lower strains in the deeper part of the ROI. This may be an effect of stress attenuation or caused by firm material boundary conditions.

Real-Time Elastography (RTE) images the relative difference in tissue hardness by measuring local strain in soft tissue. The algorithm uses consecutive RF frames and combines tissue Doppler and the enveloped RF-signal [16]. This allows tracking of small

and larger changes in echo positions without aliasing. This algorithm is referred to as the Extended Combined Autocorrelation Method (ECAM) [17]. The method allows strain mapping in both the axial and the lateral direction. The strain image resolution in the axial direction is defined by overlapping reading frames. The density of scan-lines defines strain resolution in the lateral direction, and is generally lower than the axial resolution. The method does not track tissue movement in the elevational direction. RTE was the autocorrelation method applied for strain imaging in this thesis.

1.4.2 Vibro-acoustic elastography

Vibro-elastography (VE)

By creating a tissue vibration with acoustic frequencies of 10-50 Hz, tissue strain may be recorded by ultrasonography. Clinical images of the prostate have been acquired using a low frequency (<20 Hz) broadband vibratory motion with small amplitude in order to image prostate tissue viscosity and stiffness trans-rectally [18]. This method has also been compared to MRI images of prostate and showed improved 3D representation as well as better imaging of viscoelastic properties.

Vibro-acoustography (VA)

The method referred to as vibro-acoustography (VA) [19] uses US radiation force by applying simultaneous focused intersection of two US frequencies of slightly different frequency (E.g. f 1=3.00 and f 2=3.05 MHz). The resulting acoustic wave has a frequency of $\Delta f = f1 - f2 =$ 50-60 KHz. It propagates nonlinearly and may be tracked for analysis of tissue mechanical properties. The method has been able to produce speckle-free images of prostate and breast tissue, with improved imaging of tumours, calcifications and borders [20]. VA has been implemented in a commercial US scanner as a prototype (GE Vivid 7) [21].

1.4.3 Shear wave elastography

Shear waves are qualitatively different from waves caused by compression/decompression. A shear wave may be created as a result of an indentation of soft tissue or perpendicular to compression/decompression waves (acoustic waves) propagating through a medium.

Shear waves appear in the kilohertz range (75-600KHz) and travel at a much slower speed than compression waves, typically in the range of 0-10 m/s in biological tissue. The propagation speed is dependent on the shear wave frequency [22]. The Shear modulus, μ is related to the propagation speed of shear waves c_{sw}:

$$c_{sw} = \sqrt{\mu/\rho}$$

where ρ represents the material density [23].

The relation ship between Elastic modulus (E) and shear modulus (μ) can be expressed as [24]:

$$\mu = \frac{E}{2(1+\upsilon)}$$

where υ represent Poisson's ratio. For soft tissue υ can be approximated close to 0.5 because soft tissues can be considered incompressible. Using this approximation in the equation above, the relationship between Shear modulus and Elastic modulus can be considered as:

$$\mu \approx \frac{E}{3}$$

According to this, Elastic modulus (E) may be determined by shear wave propagation speed (c_{sw}) according to the following equation:

$$c_{sw} = \sqrt{\frac{E}{3\rho}}$$

Tracking of shear wave propagation speed has been used to map tissue elasticity both qualitatively and quantitatively using the assumptions presented above [22,25-31].

Transient Elastography

In transient elastography, a push-pulse shear wave is transmitted transiently and the propagation is tracked using ultrasound. For clinical purposes, the measurement of liver tissue stiffness has been demonstrated [27-29,32]. Fibroscan® (Echosens, France) contains a patented US transducer with an indentation piston enabling shear waves travelling into liver tissue [33]. US is utilised to follow the shear waves, and measure the shear wave travelling speed. The tissue elasticity is related to shear wave speed as shown earlier, and the quantification is given in kPa [34]. The Fibroscan® is specifically made for liver tissue hardness measurements, and is not a regular US scanner providing high-quality anatomical images. However, the application is easy to learn, and the examination does not rely on experience in ultrasonography. The scanner has proved good ability to distinguish between substantial fibrosis (≥Metavir score 2) and low fibrosis (<Metavir 2) in several studies [28,35,36].

Acoustic Radiation Force Impulse (ARFI)

Acoustic radiation force impulse is used to create deformation, and a shear wave is tracked in a selected area of the tissue. The shear waves are created perpendicular to the axial direction of a focused US beam. The quantification of tissue hardness is obtained by recording shear-wave speed, where higher speeds indicate harder tissue [37]. The focused exciting US beams are transmitted only when released by the observer, and with intervals allowing cool-down of the US probes. The ARFI system is commercially available in Siemens 2000 scanners under the name Virtual Touch quantification (VTq). Mean shear wave speed is recorded in a limited ROI of 10 x 5 mm. The system is available in both linear and curvilinear external probes. It has been applied in a number of clinical settings relevant for gastroenterological imaging and elastometry including endocavitary probe, liver lesions and for other tissue characterizing purposes in gastroenterology [25,26,38,39]. A further development of the ARFI method was introduced in 2009 using laterally spaced sequential push pulses followed by a series of reading pulses. This method, called Spatially Modulated Ultrasound Radiation Force (SMURF) makes use of recording the shear

wave frequency lateral to the push pulses, and validation studies have been performed [40,41].

Supersonic Shear Imaging (SSI)

Supersonic Imaging is a shear wave imaging (SWI) method where a series of acoustic signals are deposited subsequently with focus at different depths in the tissue. This creates a plane shear wave travelling as a "mach-cone" orthogonal to the acoustic pressure waves. The method records up to 5.000 frames per second allowing a detailed tracing of the shear waves. The local shear wave speed is recorded and presented as a colour map over the B-mode image [42,43]. Several "mach-cones" are produced parallel in the tissue, reducing the impact of shear-wave attenuation. This method provides a qualitative strain map and quantitative approximation of tissue elasticity provided in kPa for any selected area in the ROI. It has been demonstrated for liver tissue scanning [30,44] and for breast [45]. The potential for viscoelastic imaging of tissue elements by tracking the phase velocities for different shear wave frequencies has also been proposed [22]

1.4.4 Strain rate imaging (SRI)

Strain rate imaging is useful for studying contracting organs such as muscles, heart and the GI tract. In strain rate imaging the endogenous deformations in muscle tissue can be tracked over time. The strain rate is the temporal derivative of the strain. While strain gives a measure of the amount of deformation, the strain rate indicates the rate of deformation. During elongation of tissue, the strain rate is positive and during contraction it is negative. If no strain occurs, the strain rate is 0. This may give a unique imaging of contractions and relaxation useful in functional diseases. Strain rate is recorded by speckle tracking methods using tissue Doppler [46,47]. This method has some limitations due to angle dependency and aliasing [48]. While tissue velocity imaging has been particularly developed and validated in cardiology [49,50] also slower moving organs such as the motility of the gastrointestinal tract have been imaged using this method [51,52]. In the latter application SRI was found to be more accurate in the radial than in the circumferential direction [53]

2. Aims of the study

The aim of the present thesis was to test the following hypotheses:

H1: Real-Time Elastography can image differences in elastic contrasts in soft tissue.

H2: Real-Time elastography can differentiate between malignant and benign lesions in soft tissue.

3. Materials and methods

3.1 Phantom studies

Study number 1 and the main part of study number 2 were performed on a tissue-mimicking (TM) phantom designed for elasticity imaging. Several materials were considered for use in the studies. An advanced method for making anthropomorphic phantoms using different concentrations of safflower oil dispersed in a gelatine suspension was described by E. Madsen et al.[54]. Polyvinyl alcohol cryogel (PVA-C) increase in stiffness by repeated freeze and thaw cycles, and has been used to document elastography methods [55]. The combination of similar amounts of gelatine with variable concentrations of agar and oil dispersion seems to simulate more realistic non-linear tissue elasticity [56]. The ideal material for elastography measurements should mimic both the acoustic properties (speed of sound, speckle) and viscoelasticity (poroelastic material) with elasticity range mimicking that of healthy and diseased soft tissue. Such material with a reasonable stability over time and durability in storage and transportation does not exist according to our knowledge. We decided to use a commercial elasticity phantom from CIRS (CIRS Model 49, CIRS Inc. North Carolina, USA). This phantom is made of a patented polymer, Zerdine®. The material has stable acoustic qualities, speckle and speed of sound [57]. It is an elastic material, but it does not have the viscoelastic properties found in real biological tissue. In our phantom the background material did not have free borders, but was encased in a stiff plastic box. Zerdine phantoms have long durability, and the inclusions, which are isoechoic compared to the background material, are individually quality-assessed by the producer in every phantom.

3.2 Patients

3.2.1 Study 2: Healthy liver tissue imaging

One healthy individual gave consent to transcutaneous US with elastography of normal liver tissue after oral information.

3.2.2 Study 3: Neoplastic and inflammatory bowel wall lesions

Cancer in the colon, rectum and anus has a combined annual incidence of approximately 3600 in Norway and is thus one of the most common cancers [58]. The disease is most commonly diagnosed from the 6th to 8th decade of life. Survival is related to the tumour and nodal status as well as the presence of distant metastases. Colorectal cancer growth starts in the mucosa and gradually involves the submucosa, the proper muscle layers and eventually the adventitia or the serosa layers of the bowel. Crohn's disease is a transmural inflammatory bowel disease, which may form skip-lesions in the whole GI tract, but predominantly in the terminal ileum. The disease had an incidence of 5.8/100.000 per year in south-east Norway in 1990-93 [59] and increasing incidence has been documented for Europe [60] and North America [61] over the last decades. Crohn lesions and neoplastic lesions are usually distinct in their clinical presentation, but histology is used to rule out carcinoma or high-grade dysplasia, especially in the presence of colon or rectal affection. In our study, we wanted to compare Crohn- and neoplastic lesions as a model for benign and malignant lesions in the same organ (bowel wall). 39 patients scheduled for surgery for Crohn's disease or for neoplastic tumours in the small or large bowel were included. The patients accepted that their surgical specimen would be subject to ultrasonographic examination with elastography prior to formalin fixation and subsequent pathological examination.

3.2.3 Study 4: Pancreatic focal lesions

Focal pancreatic lesions may represent benign or malignant disease. In case of malignant lesions the survival is significantly better for localised disease compared to total group survival in both men (18.7% vs. 4.9%) and women (15.9% vs. 3.1%) according to Norwegian data from 2005-09 [58]. In a study of 288 pancreaticoduodenectomies performed in a Dutch referral centre for pancreatic surgery in 2000-2009, 36 (13.1%) resected lesions were retrospectively found to be benign entities. Twenty-three (8.4%) cases showed benign, non-neoplastic lesions

and 13 (4.7%) lesions were benign neoplasms [62]. Improved preoperative diagnosis may reduce the number of pancreaticoduodenectomies for benign lesions.

43 patients were invited to participate in a clinical study with EUS elastography in order to examine a focal lesion located in the pancreas. Patients with previous imaging indicating progressive malignant disease with metastases or locally advanced tumours were not included. In 15 patients EUS guided Fine-Needle Aspiration (FNA) was performed. 21 patients underwent surgery, 2 non-operated patients had positive EUS-FNA cytology and 25 patients were followed up according to clinical practice including repeated imaging.

3.3 Endoscopic ultrasonography (EUS)

EUS is an endoluminal examination where the US probe is inserted under endoscopic guidance into the gastrointestinal tract [63-65]. EUS may be performed with miniature probes that can be inserted through the working channel of standard gastro- or colonoscopes [66-68]. Larger areas can be imaged using dedicated echo-endoscopes, which have an US probe mounted at the tip of the scope [69]. New electronic instruments combine the endoluminal imaging abilities of video-endoscopes with ultrasonography in the range of 5-12 MHz including Doppler facilities for imaging of blood vessels. The probes may be radial providing a 360 degree US image of the circumference or curvilinear, providing a scan plane parallel to the scope axis in prolongation of the working channel of the endoscope. The latter option also allows US-guided interventions such as FNA or needle-biopsies to be performed through the endoscope [70-72]. In study 4, a curvilinear echo-endoscope (Pentax EG 3870 UTK) compatible with an US scanner with Real-Time Elastography (Hitachi Hi Vision 900) was used. One of the unique features of EUS is the close proximity to mediastinal, retroperitoneal and intramural lesions enabling use of high frequency US with relatively limited amount of artefacts and a high spatial and temporal resolution.

3.3.1 EUS guided tissue sampling

EUS-guided tissue sampling is possible using a curvilinear echoendoscope [73]. Single-use needles for fine-needle aspiration (FNA) or tru-cut biopsy were passed, usually several times, through the working channel of the endoscope and inserted into a pathological lesion under the visual control of the examiner. Material from FNA needles was prepared on glass slides for immediate evaluation by a cyto-technician. If the material was not representative, another needle pass was attempted. The cyto-technician only indicated whether the material was representative and gave no indication of cellular morphology or diagnosis. When lesions extended 2 cm in diameter, a tru-cut biopsy (Quick-core, Cook) was attempted. If no material was obtained we performed a subsequent FNA. Core biopsies were placed in formalin and sent directly to histology without microscopic evaluation in the examination room. If patients were planned for pancreatic surgery, tissue sampling was usually not performed. In all cases where post-operative histology or intra-operative tru-cut biopsies were obtained, they were used to define the final diagnosis.

3.4 Strain image evaluation methods

3.4.1 Visual categorical score (VCS)

Several categorical score systems for visual evaluation elastography images have been proposed. Most of them are focused on strain distribution within the lesion. The first score was introduced by Dr.Itho for evaluation of breast lesions [74], this 5-point Likert scale, also referred to as the Tsukuba score, has been model to several other elastogram scores for other clinical applications. For pancreatic lesions, a similar 5-step score was proposed [75]. A more complex elastography score in pancreatic lesions was proposed by Janssen et al. taking into account both the representation of colours and their patterns of distribution within focal pathological lesions, in pancreatitis and in healthy pancreas [76]. In study 3 and 4, we have applied this score system. The advantage of a VCS is simplicity in use and straightforward comparison between observers in the same cases. Disadvantages of VCS include the subjectivity

of the method, sensitivity to individual differences in colour-vision, that categories of a defined scale may not fit well with the actual findings and that the image categories may not correspond well with pathological processes. For the distinction between malignant and benign disease, lesions classified in the mid-scale may be difficult to classify.

3.4.2 Visual Analogue Scale (VAS)

Visual Analogue Scale is a method used for semi-quantification of subjective perceptions and is frequently used for perceptual sensations such as pain [77], itch [78], nausea [79] or fatigue [80]. In comparative studies VAS scores have shown better reproducibility than categorical scales [81]. We applied a 100 mm horizontal line without scaling and the observer set one mark indicating the supposed lesion hardness as compared to the surrounding tissue. Softer lesions were indicated to the left, no difference from surrounding tissue was indicated mid-scale, and harder lesions from the middle to the right end. Advantages of the VAS score include that it is intuitive and easy to use and it provides a value based on a linear scale allowing further statistical analysis of the data. A disadvantage may be that it is not well suited for describing more than one quality at the time (e.g. colour content and pattern distribution). As a semi-quantitative score it may also have low reproducibility because different observers may apply the scale differently. In our studies, the VAS scoring included a comparison of lesion strain to strain in surrounding tissue (reference tissue), while the VCS was solely based on lesion strain pattern.

3.4.3 Strain Ratio (SR)

SR is the ratio between mean strain in a reference area (B) and the mean strain in an area within a lesion (A). By directing the fraction as B/A, hard lesions (with low strain) compared with softer reference tissue (with higher strain), will produce increasingly higher SRs for tumours of increasingly higher hardness relative to the reference area (elasticity contrast). If there is no difference in mean strain in selected reference and tumour areas, SR is 1.0. A main advantage of SR is the automated procedure incorporated in the scanner software, which allows this a presumably more

objective measurement on frozen single images during the scanning. Several frames from a single cine-loop can be measured, and a mean or median SR value may be found for each inclusion. SR provides a quantitative measurement of strain differences (elastic contrast) based on an assumption that both of the compared areas are subject to the same amount of stress. Limitations of the method include that the selection of frames for comparison within the lesion and reference tissue, is user-dependent. Selection of unrepresentative elastograms or reference tissue with different distance to the stress source may bias the method and lead to large measurement variability. This may be particularly important in complex, heterogeneous tissues where dampers and sliding surfaces are present and the source of stress is not precisely located.

3.5 Ethics

All studies that involved patient examinations or use of surgical specimens from patients were approved by the Regional Committee for Ethics in Medical- and Health Science in Western Norway and were conducted according to the Helsinki Declaration. Study 4, on pancreatic focal lesions by EUS, was also registered as a prospective clinical trial at: clinical.trials.gov with reference number NTC 01360411.

All patients invited to participate received oral and written information about the study. They were informed that participation was voluntary and that they could decide to withdraw their consent at any time. Only one patient in study 4 decided to withdraw her consent.

3.6 Statitical methods

3.6.1 Linear or log-scale for strain ratio (SR)

A linear scale for SR is good for recognition for other users of this measurement. However, this ratio is designed to give softer lesions a SR between 0-1 and harder lesions a SR >1. For harder lesions, representing a certain elastic contrast the SR

measurements frequently can be found in a range of 5-100. The harder the lesions, the higher the SR variability [82]. This is frequently due to a very low denominator in the ratio B/A when strain in lesion (A) becomes very small. If SR is expressed as a log scale, the visibility of small changes in the range of 0-1 is maintained, while the variability of larger SR measurements is less pronounced.

3.6.2 Intra- and interobserver agreement

Cohen's kappa

Cohen's kappa is a statistical measurement of the reproducibility of a test using a categorical variable. The test can be used to measure the performance of the same observer at two different times or between two different observers. Cohen's kappa expresses the degree of agreement surpassing the agreement observed by chance. $\kappa=1.0$ expresses complete agreement, while $\kappa=0$ expresses the agreement expected by chance. If agreement is lower than expected, the κ value will become negative. Interpretation of the κ value is often regarded as: $\kappa>0.81$: Very good agreement, $0.61<\kappa<0.80$: Good agreement, $0.41<\kappa<0.60$: Moderate agreement, $0.21<\kappa<0.40$: fair agreement and $\kappa<0.20$: Poor agreement [83].

Intra- and interclass correlation (ICC)

Intraclass correlation coefficient (ICC) quantifies measurement error in a numerical (continuous) variable. The test is the ratio between variance of the underlying values between individuals to the variance of observed values. The test expresses the measurement error relative to the true variation between individuals. The smaller the amount of measurement error, the smaller increase in variability of observed values, and the closer ICC will be to 1.00. We have used the expressions Intraclass correlation for intraobserver variation and Interclass correlation for interobserver variation.

Correlation

Correlation is a measure of association between two recordings of continuous variables. We have used this to evaluate scorings recorded by two examiners using the same continuous scale or from the same examiner using the same method at two

different points in time. A correlation coefficient, *r* expresses the scattering of the data around an underlying linear trend. *r* can vary between -1 to +1. For normally distributed data we have used Pearson's correlation. For non-normally distributed data we have used Spearman's correlation (rank correlation).

Limits of agreement

Limits of agreement express the difference between individual measurements to a common mean value of two observers or between repeated measurements by the same observer at two different times. The method is useful for measuring repeatability of a single measurement method or to assess separate measurements performed by two observers. The Limits of Agreement plot provides information about the deviation of the mean difference (*d*) representing variability in applications of the scale. Based on the standard deviation of the difference we have plotted the 95% Confidence Interval (CI) to give an impression of the test's reproducibility. The plot can also disclose if variation in difference (*d*) is unevenly distributed along the scale used, e.g. higher differences for higher values. The differences (*d*) may often have a normal distribution even if the measurements do not. If this is the case, 95% of the measurement differences will be within the calculated CI [84].

Generalized Estimating Equations (GEE)

Data in study 3 and 4 arise from studies on individual lesions in different subjects, but also from separate lesions in the same subjects (e.g. multiple Crohn lesions, tumours in surgical specimens and separate pancreatic lesions in one patient). This represents clustering of data. Analysing data in a regression analysis without taking clustering into account may lead to smaller standard errors and narrower confidence intervals, with corresponding p- values being too small. In our data the clustering of 2-3 lesions in some of the patients had no intrinsic interest, but was rather a nuisance. The GEE model provides parameter estimates and standard errors corrected for such clustering. The model provides estimated marginal means of parameters and confidence intervals [85].

3.6.3 Receiver operating Characteristic (ROC)

A Receiver Operating Characteristic curve can be used to illustrate the performance of a diagnostic test using a continuous variable for the detection of positive or negative cases (dichotomous outcome). The curve represents different cut-off values for the diagnostic test represented by the corresponding sensitivity and specificity. In order to construct a ROC curve, the diagnostic test must be compared to a gold standard. In our studies, this has been histology, cytology or follow-up. The ROC curve, frequently presented as 1-specificity on the first axis, and sensitivity on the second axis, visualise the test performance at different cut-off values in individual lesions. The area under the ROC curve expresses the overall accuracy of the test. Sensitivity of a test is defined as the proportion of true positive tests divided by true positive tests + false negative tests. Specificity of a test is defined as the proportion of true negative tests divided by true negative + false positive tests. Sensitivity and specificity have an inverse relationship.

4. RESULTS AND SUMMARY OF PAPERS

4.1 Paper 1

Freehand Real-Time Elastography: Impact of Scanning Parameters on Image Quality and In Vitro Intra- and Interobserver Validations

Background: Real-time elastography is a method for visualization of the elastic properties of soft tissue and may potentially enable differentiation between malignant and benign pathologic lesions. Our aim was to validate the method on a tissue-mimicking phantom containing eight spherical inclusions with known storage modulus and to evaluate the influence of different scanning parameters and investigator variability. Two investigators performed series of standardized elastography scans applying a 5-step categorical quality scale to evaluate the influence of 7 parameters: dynamic range of elasticity, region of interest, frequency of transducer movement, rejection of elastogram noise, frame rate, persistence and smoothing. Subsequently, examinations of 4 selected inclusions were performed using a visual analogue scale (VAS) representing the span in image quality.

Results: The inclusions with higher elastic contrasts were imaged more clearly than the inclusions with low elastic contrasts. Intra-observer agreement using the categorical scale on elastogram quality was good (kappa: 0.67 to 0.75) and inter-observer agreement moderate (kappa: 0.55 to 0.56). The subsequent VAS evaluation gave intraclass-correlation coefficients for the two observers of 0.98 and 0.93, respectively, and an interclass-correlation coefficient of 0.93. Dynamic range of elasticity was the parameter with most impact on the elastographic visualization of inclusions.

4.2 Paper 2:

Real-Time Elastography: Position of Reference Area influences Strain Ratio Measurements

Strain ratio (SR) is a semi-quantitative measurement of strain differences between two user-defined areas in an elastogram. The aim of this study was to evaluate the impact of size and location of reference area when measuring SR of focal lesions in a tissue-mimicking phantom and in normal liver tissue. We also interrogated impact on SR by the scanner parameter Elasticity dynamic range (E-dyn). Two investigators individually collected data by scanning 4 spherical inclusions with known storage modulus different from the background. Subsequently, a liver scan was performed in-vivo using the same scanning protocol. Five different setups with changes in position or size of reference areas were tested. All eight levels of the scanner setting E-dyn were recorded for each setup and SR was measured in 3 different representative elastograms for each recording situation.

Results: The four inclusions representing different elastic contrasts had significantly different mean SR levels ($p<0.01$) when the background material was used as reference. Changing the position of the reference area to a deeper position influenced the measurements of SR significantly for all phantom lesions and in a healthy liver. Changing the size of the reference area, while keeping the centre depth unchanged, did not influence mean SR levels significantly. SR was independent of the E-dyn parameter setting. Intra- and interobserver reliability was high when measuring SR with a free-hand technique. The lowest interobserver correlation was found when the reference area was positioned superficially to the lesion (ICC=0.851). The best interobserver correlation was found when the reference area had similar size and distance from the probe as the inclusion area (ICC=0.985).

4.3 Paper 3

Strain Assessment in Surgically Resected Inflammatory and Neoplastic Bowel Lesions

The purpose was to investigate if ultrasound-based strain imaging could discriminate between lesions of colorectal adenocarcinomas and Crohn's disease in newly resected bowel specimens. Twenty-seven patients electively operated for colorectal tumours or stenotic lesions from Crohn's disease were prospectively examined with ultrasonography using a Hitachi HV 900 US scanner with RTE. Three different methods were applied to assess tissue strain: A visual categorical score (VCS), a continuous Visual Analogue Scale (VAS, 0-100) and Strain ratio (SR) measurement between the lesion and surrounding reference tissue. The imaged sections were marked and subsequently examined by a pathologist. Results from RTE were evaluated according to diagnosis, degree of fibrosis, inflammatory parameters, tumour stage and grade.

Results: Sixteen sections from Crohn-lesions, 18 sections from adenocarcinomas and 4 sections from adenomas were examined. Both adenocarcinomas and Crohn-lesions were found to be harder than surrounding tissue, but they could not be discriminated from each other by any of the strain imaging evaluation methods. All adenocarcinomas had significantly higher strain ratios than adenomas. VCS differentiated poorly between Crohn-lesions, adenocarcinomas and adenomas. Tumour stage or grade did not have significant impact on elastography results.

4.4 Paper 4

Characterisation of Focal Pancreatic Lesions using Endoscopic Ultrasonography with Real-Time Elastography

The aim of this study was to apply RTE endoscopically on pancreatic lesions representing unknown aetiology and to evaluate its efficacy in differentiation between

malignant and benign lesions and if possible, establish other diagnoses more precisely. Forty-eight pancreatic lesions in 39 patients were successfully included prospectively over a 3-year period. Three strain evaluation techniques were used: 1: Strain ratio (SR), 2: continuous Visual Analogue Scale (VAS) 3: A visual categorical score (VCS) based on the lesion's colour distribution. Final diagnosis was based on histopathology (21), positive FNA cytology (2) and/or follow up (25) for 6-25 months.

Results: Real-time elastography performed during the EUS evaluation of pancreatic solid lesions showed a significant difference between groups of benign and malignant lesions using SR and VAS. A ROC curve analysis on the ability of median SR to distinguish between malignant and benign lesions found a sensitivity and specificity: 67% and 71.4% for a cut-off of SR = 4.4 (ROC-AUC: 0.814). For VAS the best sensitivity and specificity was 100% and 82% for cut off: 87.5 (ROC-AUC: 0.869).
Two benign microcystic adenomas had higher median SR values than malignant lesions. The measurement variability was substantial and the ROC curve indicated a limited accuracy for SR in endoscopic RTE evaluation of focal pancreatic lesions. A combination of VCS categories gave a sensitivity, specificity and accuracy of 100%, 61% and 76% for differentiation between benign and malignant lesions. Some categories were only used for benign lesions.

5. GENERAL DISCUSSION

5.1 Relevance of strain measurement in biological tissue

Established imaging modalities such as ultrasonography (US), Computed Tomography (CT) and Magnetic Resonance Imaging (MRI) make use of acoustic impedance, absorption of X-ray radiation and temporal changes in molecular magnetic orientation, respectively. Strain imaging images elastic properties in soft tissue, and it has been assumed to have the potential to improve differentiation between malignant neoplastic tissue and other disease entities. The basis for this hypothesis is the clinical experience that malignant tumours in many soft tissues frequently become much harder than the healthy tissue.

The basis for tissue hardening in neoplasms is partly understood and is probably an effect of two major pathophysiological processes, desmoplasia and increased interstitial pressure. Desmoplasia is a process involving increased activity of fibroblasts resulting in marked fibrosis within, and sometimes in the vicinity of malignant tumours [86,87]. Desmoplastic reaction has typically been described in adenocarcinomas of the breast and the pancreas [88-91]. Increased interstitial pressure has also been found in malignant tumours [92-94]. This has been investigated primarily from the perspective of pharmacodynamics, where increased interstitial pressure has been a limiting factor in obtaining adequate drug concentration within malignant tumours [95,96]. In a study on ARFI imaging in patients with acute resolving pancreatitis Mateen et al. observed a reduction in shear wave velocity within few weeks after acute pancreatitis, probably reflecting the resolving oedema [97]. Using elastography as a diagnostic imaging technique, both desmoplasia and increased interstitial pressure may contribute to the result. The relevance of elastography for characterisation of biological tissue is based on the uniqueness of these features in diagnostic entities and whether the images can reliably be reproduced.

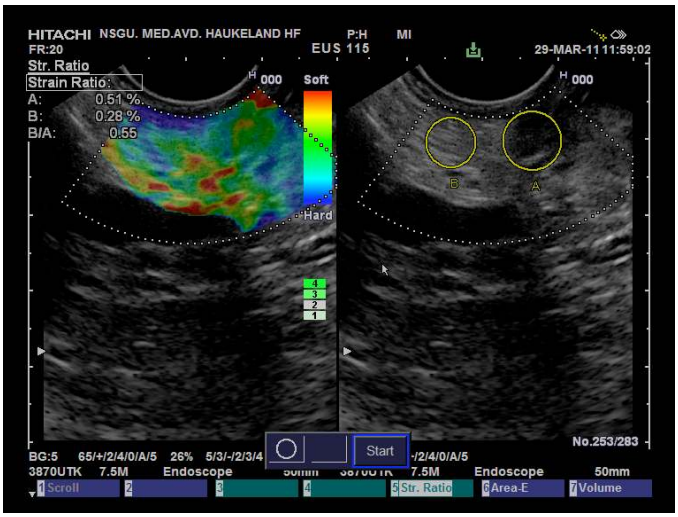

Figure 3: Endoscopic elastogram (left) and B-mode sonogram of a solid, hypo-echoic lesion in the body of the pancreas. The lesion is being measured with strain ratio marked on the B-mode image (right); dividing mean strain in circle B (reference) with mean strain in circle A (lesion) yields a SR of 0.55, indicating that the lesion is softer than the pancreatic reference tissue. Diagnosis after follow-up: Sequelae of pancreatitis.

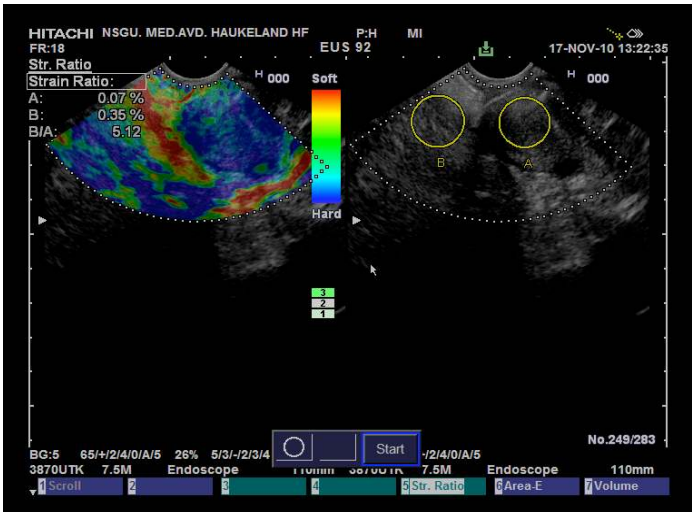

Figire 4: Endoscopic ultrasonography with RTE shows an adenocarcinoma in the pancreas. Elastogram (left) shows blue colour indicating low strain corresponding to hypoechoic tumour tissue in B-mode (right). A strain ratio between reference (circle B) and tumour tissue (circle A) yields a SR of 5.12.

5.2 Limitations of the elasticity phantom

The elasticity phantom used in this thesis is a commercial phantom made of a synthetic polymer, Zerdine® (CIRS, Elasticity QA phantom, Model 049, Virginia, USA). The phantom had been individually validated for speed of sound, US attenuation, storage moduli (elasticity) of background material (30 kPa) and inclusions (9,15,39 and 57 kPa). The phantom material had solely elastic properties and did not mimic the viscoelastic properties of real soft tissues. The inclusions were within the range of elasticity contrasts observed in biological tissues examplified by breast and prostate, although some researchers have reported much higher elastic contrasts for some malignant lesions [15,98].

The phantom material was also embedded in a solid plastic box restricting free movement of tissue- mimicking material towards the edges, and probably influencing strain measurements, particularly near the lateral edges of the phantom. This issue may also apply to clinical elastography as many organs are tightly embedded in connective tissue structures, or their movement may be variably restricted in different directions depending on their neighbouring organ tissue structure [99]. McAlveary et al. used Zerdine phantoms with shear modulus 2.7-18 KPa embedded in PVC cylinders for validation studies of Spatially Modulated Ultrasound Radiation Force (SMURF) and evaluated the same uncovered phantoms in unconfined compression testing. They found very similar and reproducible shear modulus measurements by SMURF compared to compression testing [40].

5.3 Limitations of ex-vivo tissue elastography

As mentioned previously, interstitial pressure contributes to properties recorded in the elastography image. This feature is more transient than the structural changes caused by proliferation and recruitment of fibroblast and subsequent collagen production. Interstitial pressure may be influenced by blood pressure, albumin level or other osmotic substances in circulation [100]. When excised tissue is used as the study object, the contribution from interstitial pressure will be lost within minutes. Hence,

ex-vivo elastography of biological tissue only image changes in tissue-strain due to desmoplasia.

5.4 Complexity of free-hand strain imaging in vivo

In contrast to a laboratory situation with control over pressure exerted by a fixed probe in a stepping motor on a near homogeneous material without encasement, the clinical situation introduces a large increase in complexity and possibilities for corruption of the strain signal when performing elastography. The introduction of free-hand scanning allows variability in pre-compression level and in cyclic compression and may influence the strain image. The position of the stress source relative to the ROI is also essential in order to interpret the elastogram. Tissue stress as well as the corresponding strain tends to decrease with increasing distance from the stress source. Knowledge about the position of the stress source and the corresponding strain field is important in order to perform SR measurements within the ROI. The elastogram may be corrupted by intersection of dampers of strain such as large veins, which absorbs the strain and make the adjacent tissue appear harder. Arteries may act contrary, as they make up a local strain field in their circumference where the tissue may appear softer due to increased strain. Another confounder of strain imaging is the intersection of the ROI by a peritoneal surface or other anatomical plane allowing a translational tissue movement e.g. as a result of breathing or local pressure. Along these planes, the elastogram based on autocorrelation strain imaging methods will display a strong high-strain signal, indicating normal translational movement in the same manner as for very soft tissue. In the following table, some of the favourable and non-favourable factors in clinical Real-Time Elastography are summarized according to our experience with clinical application of the method both endoscopically and transcutaneously.

Table 1: Factors influencing soft tissue strain-imaging

Factors enabling more reliable clinical Real-Time Elastography imaging	*Factors contributing to less reliable clinical Real-Time Elastography imaging*
Close proximity of target to stress source (1-3 cm)	Distance between stress source and target (>3-4 cm)
Near homogeneous tissue (e.g. liver)	Inhomogeneous tissue
No intersection of peritoneal planes or other anatomical planes allowing free slip movement in the ROI	Intersection of peritoneal planes or other anatomical planes allowing free slip movement in the ROI
Some distance to tissue boundaries	Close proximity to tissue boundaries
No dampers present (e.g. large veins)	Dampers present in ROI
Probe or balloon used as stress source	Endogenous stress source
A broad stress source relative to the ROI	A narrow stress source relative to ROI
Knowing the position of the stress source relative to the ROI	Not knowing the position of the stress source relative to the ROI
A limited number of diagnostic entities	A large number of possible diagnostic entities

In a preoperative study of rectal tumours, an accuracy of 0.94 was obtained using SR for the distinction between malignant and benign lesions in a study of 69 patients [101]. In this study, a rectal probe was used with a balloon providing pulsatile stress operated by the observer, acting as a 360-degree stress source. The lesions were close to the probe, yet the balloon would allow some spacing and pre-compression on the tissue. There were no intersecting large vessels or peritoneal surfaces, and the diagnostic possibilities were essentially only two: Adenoma or adenocarcinoma.

In our study on pancreatic solid lesions (study 4) using EUS Real-Time Elastography with SR evaluation, we obtained ROC-AUC of 0.81. In this study, we utilised endogenous stress sources, sometimes out of the scanning plane for the lesion and probably involving individual variability due to pulsatile blood pressure and aorta compliance. We used a curve-linear probe (echoendoscope) where the probe area was narrower than ROI of the elastogram in many cases. Frequently, vessels were included in the ROI producing strain-absorbing areas near or in the pancreatic tissue. Finally, the possible diagnostic entities were several: adenocarcinoma, malignant neuroendocrine tumour (NET), benign NET, adenoma, serous microcystic adenoma, focal pancreatitis and other benign lesions. All these factors can in part explain why the ability to differentiate benign and malignant lesion seem less accurate in the pancreatic than in the rectal study.

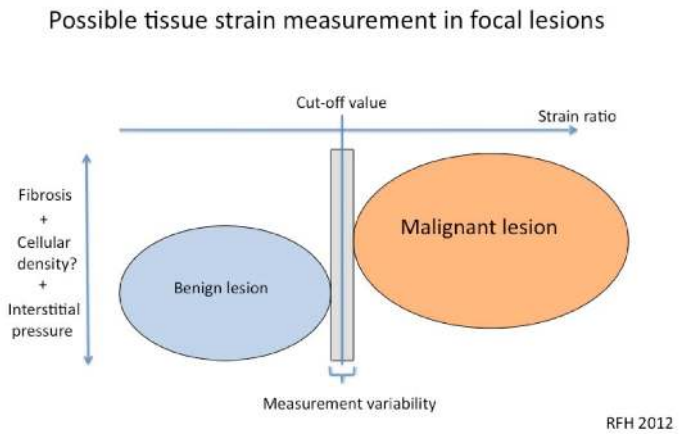

Figure 5: An ideal hypothetical (H2) differentiation between malignant and benign lesions based on semi-quantitative elastography using SR. A cut-off value with limited measurement variation enables complete separation of malignant and benign lesions. On the left: contributing factors to tissue strain differentiation.

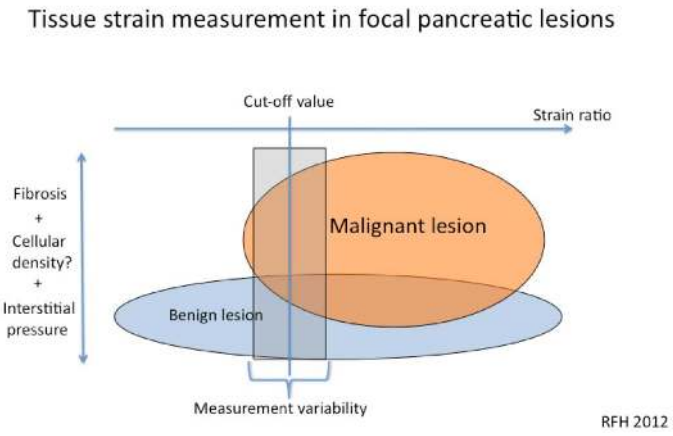

Figure 6: A more realistic scenario of differentiation of focal pancreatic lesions based on the results from our EUS elastography study on apparently solid pancreatic lesions. Our findings suggest a larger overlap in strain between malignant and benign lesions and that SR as a semi-quantification technique have substantial measurement variability that implement on reliability. Possibly, the SR cut-off value can be set low in order to exclude malignant lesions at the cost of a larger number of false positives.

5.5 Other clinical studies on EUS elastography of focal pancreatic lesions

Several other groups have studied EUS elastography of solid pancreatic lesions. The prevalence of malignant lesions in these study populations is in the range of 60-80%, which is higher than in our material and favours the positive predictive value of a harder lesion. Different studies cannot be compared directly because they have used different evaluation of the qualitative elastogram. To date only two studies by J. Iglesias-Garcia et al. [102] and F. Itokawa et al. [103], respectively, have used SR as the strain evaluation tool. The evaluation of 109 focal lesions by F. Itokawa et al. was performed using Giovannini's visual scale [75]. A post-hoc analysis included 7 lesions confirmed as mass-forming pancreatitis with mean SR 23.77(12.65) and 72 adenocarcinomas with SR 39.08 (20.54). They found a significant difference between the groups using T-test. The other lesions examined representing non-mass forming chronic pancreatitis (n=6), autoimmune pancreatitis (n=7), neuroendocrine tumours

(n=9) and normal pancreatitis (n=8) were excluded from the SR analysis. The analysis also showed large overlap between individual lesions of each entity, and large standard deviation of approximately 50% of the mean SR value for each entity. Evaluating the categorical score, 23 cases with score 3 were defined as inconclusive and excluded from further analysis. Based on score 1+2 as benign and score 4+5 as malignant, they reported a sensitivity of 0.99 and a specificity of 0.64. However, since 21% of the examined lesions were found inconclusive and excluded from analysis, these numbers are difficult to compare with other studies.

J. Iglesias-Garcia et al. published a material of 86 patients with focal pancreatic lesions, including 58 (67%) malignant tumours, where SR was used for evaluation. In this paper, the area with highest strain (softest) was consequently used as reference tissue. The depth of the reference tissue relative to the tumour tissue was not standardised. From our point of view, this approach did not sufficiently take into account the effect of strain attenuation and other strain increasing artefacts along planes of natural translational movement. The use of a reference area much smaller than the lesion area also increases the likelihood of sampling error.

The following table summarizes some of the major studies performed with EUS-based elastography on focal pancreatic lesions and their method of evaluation. The most common feature is the low specificity and relatively high sensitivity in separating malignant from benign lesions. This may be explained in part by a relatively high prevalence of malignant lesions in most materials (60-82%) and a tendency of reduced strain in both malignant and benign lesions causing a high frequency of false positive cases.

Table 2: Other publications on EUS strain imaging in pancreatic disease

Author	*Year*	*n*	*Sens.*	*Spes.*	*Accuracy*	*Comment*
Giovannini et al.[75]	2006	24	100%	67%	-	Visual categorical scale (1-5)
Janssen et al.[76]	2007	53+20	93.8%	65.4%	73.5%	New visual scale 1/2/3A/B/C
Saftoui et al.[104]	2008	68	91.4%	87.9%	89.7%	Colour hue cut- off: 175/256 +Neural Network analysis
Hirche et al.[105]	2008	70+10	41%	53%	45%	Visual scale, Focal lesions, pancreatitis excluded
Giovannini et al. (Multicentre) [106]	2010	121	92.3%	80%	89.2%	Visual scale (1-5)
Iglesias-Garcia et al.[107]	2009	130+20	100%	85.5%	94%	Visual scale, descriptive: identify malignancy
Iglesias-Garcia et al.[102]	2010	86 +20	100%	92.9%	97.7%	Quantitative: Strain ratio (SR) cut off: 6.04
European EUS Elastography Multicentre study [108]	2011	258	93.4%	66.0%	AUC ROC: 0.85	Mean colour hue in lesion over several frames: 0-255, cut-off 175
European EUS Elastography Multicentre study [109]	2012	258	87.6%	82.9%	AUC ROC: 0.94	Neural Network evaluation of the same clinical material as reported above

5.6 Limitations of evaluation methods

In this thesis the qualitative elastogram representing a strain map has been semi-quantified in three different ways: Using a Visual categorical score (VCS) based on a publication by Janssen [62], a continuous visual analogue scale (VAS) based on the distribution of colours in a lesion and its surroundings and the ratio between strain in relevant reference tissue and the focal lesion (SR). With the software version used in these studies, SR had to be calculated on single frames of a recorded cine-loop. The measurements were therefore repeated several times (3-9) in the different studies. Positioning of the US probe relative to lesions and reference tissue, the frequency and the amplitude of the stress source represent basic limiting factors for strain imaging of soft tissues.

5.6.1 Visual categorical score (VCS)

This scoring system is based on the visual impression of the lesion per se and does not include evaluation of the adjacent tissue. The current RTE algorithm images strain in lesions relative to the surrounding area, and the imaged strain is dependent on the stress applied. Hence, a low strain in a lesion may be produced by hard tissue or insufficient stress. To avoid a strong bias by this mechanism, the scanner has electronic filters that suppress signals from areas with low Signal-to-Noise-Ratio (noise reject) and frames representing insufficient strain (frame reject). The VCS constituted up to 7 different categories, and particularly those involving several colours could be difficult to classify. Using the Giovannini-scale [75], some users have had difficulties with interpreting the middle category no. 3 out of 5 [103]. The categorical scale is subjective, based on individual perception of colours, which may vary. For statistical purposes categories are nominative and limit statistical evaluation of interobserver agreement to kappa statistics.

5.6.2 Visual Analogue Scale (VAS)

When applying the VAS score, the colour representation in lesion was compared to reference tissue at the same depth. As for VCS the colour perception of individual

observers may influence the evaluation. Individual differences in application of this score may also occur since it focuses on the lesion in relation to surrounding reference tissue, and hence becomes more complex than VCS. This method requires some experience with the elastogram presentation of the specific elastography application. As the scale is continuous, it allows a broader spectre of statistical evaluation including calculation of mean/median scores, cut-off values and ICC.

5.6.3 Strain Ratio (SR)

SR is less subjective than VCS and VAS score. SR is based on the condition that lesion and reference tissue is subject to a similar stress load. The selection of reference area position and representative single frames for measurement is crucial. Using the colour-map window for selecting reference and tumour area may bias the selection and involves subjectivity. SR is a continuous variable with increasing values for high elastic contrasts between hard lesions and soft reference area. Changes in lesion strain will have increased impact on measurement with higher SR values, and sometimes a logarithmic presentation of SR could be preferable. As with VAS, SR allows calculation of mean or median values and cut-off values between diagnostic groups.

5.7 Strain imaging and elasticity of soft tissue – The inverse problem

The attempt to reconstruct the elastic modulus or properties of soft tissue based on observed local strains is often referred to as “the inverse problem” [110,111] in elastography. Distribution of stress and attenuation is not likely to be uniform in a non-homogeneous, non-isotropic tissue in more than a very limited area. The distribution of stress and corresponding strain is also dependent on the boundary conditions of the tissue under examination [99]. In our studies, the boundary conditions have been different in the phantom studies, the ex-vivo studies and in the clinical application with EUS elastography of the pancreas. This may have influenced the visual evaluation as well as the SR measurements.

6. Conclusion and future perspectives

This thesis has considered two basics hypotheses concerning the application of RTE:

H1: Real-Time Elastography can image differences in elastic contrasts in soft tissue.

Our studies confirm that RTE can image differences in elastic contrast in a tissue-mimicking phantom, in resected human specimens, and in clinical examinations during EUS of the pancreas. Increasing elastic contrasts facilitates imaging, but both softer and harder lesions can be imaged with good sensitivity both in-vitro and in-vivo.

H2: Real-Time elastography can differentiate between malignant and benign lesions in soft tissue.

In a clinical study on focal pancreatic lesions, EUS-RTE showed moderate accuracy in differentiating between the groups of malignant from benign lesions. In an ex-vivo study on newly resected, devascularised surgical specimens we were not able to record any strain differences between adenocarcinomas and stenotic lesions in Crohn's disease. Both malignant tumours and chronic inflammatory changes presented with low strain indicating increased tissue hardness. Hence, the main problem with RTE seemed to be too low specificity with great strain variation, particularly in the benign entities.

RTE is currently not accurate enough to represent an alternative to diagnosis based on tissue sampling. Depending on the application, the complexity of the anatomy, position and standardisation of the stress source and the number of diagnostic alternatives, the diagnostic yield may be variable. Nevertheless, strain imaging may contribute to non-invasive diagnostic imaging as an adjunct to B-mode ultrasonography; contrast enhanced ultrasonography (CEUS) as well as other imaging modalities.

Future perspectives

Improved technology with a more standardised stress source, possibly repeated in different locations by acoustic radiation force technology, may improve strain and subsequent quantitative elasticity measurements in the future. The use of shear wave tracking for elasticity imaging has already materialized in commercially available scanners. These scanners combine qualitative strain mapping with shear wave imaging (SWI), which provide the ability to approximate Young's modulus in selected areas. This technology is still in an early phase, and more dedicated apparatus for specific elasticity measurement may be developed. SWI technology may also enable imaging of viscous properties of soft tissue.

A possible tracking of boundary conditions may be achieved by image fusion of CT or MRI, allowing approximations of stress distribution. In the evaluation of focal pathological lesions and staging of cancers, more research on the contributions from fibrosis, cellularity and interstitial pressure may be needed in order to understand limitations and for the development of specific applications. A fundamental limitation in the ability of elasticity imaging for differentiation of cancer from benign lesions, is the possible overlap in tissue elasticity between these groups as observed by tissue strain imaging in vivo.

7. Erratum

In the original version of this thesis the Acoustic Radiation Force Impulse (ARFI) method was defined as Acoustic Radiation Force Imaging in the abbreviations (p. 9) and in the description of the method (p.19). This has been corrected according to the principal literature on this method. ARFI can be used to visualise deformation as a qualitative image as well as the shear-wave based quantification described in section 1.4.3.

References

1. Ghalioungh P. Magic and medical science in ancient Egypt. London: Hodder and Stoughton; 1963
2. Wells PN, Liang HD. Medical ultrasound: imaging of soft tissue strain and elasticity. J R Soc Interface 2011;8:1521-1549
3. Odegaard S, Gilja OH, Gregersen H eds. Basic and New Aspects of Gastrointestinal Ultrasonography. 1 ed. Singapore: World Scientific; 2005:490
4. Salvesen K, Lees C, Abramowicz J, et al. ISUOG statement on the safe use of Doppler in the 11 to 13 +6-week fetal ultrasound examination. Ultrasound Obstet Gynecol 2011;37:628
5. Ophir J, Alam KS, Garra B, et al. Elastography: Imaging the Elastic Properties of Soft Tissues with Ultrasound. J Med Ultrasonics 2002;29 (Winter):155-171
6. Nasoni RL, Bowen T, Connor WG, Sholes RR. In vivo Temperature Dependence of Ultrasound Speed in Tissue and its Application to Noninvasive temperature Monitoring. Ultrason Imaging 1979;1:34-43
7. Dickinson RJ, Hill CR. Measurement of soft tissue motion using correlation between A-scans. Ultrasound Med Biol 1982;8:263-271
8. Wilson LS, Robinson DE. Ultrasonic measurement of small displacements and deformations of tissue. Ultrason Imaging 1982;4:71-82
9. Ueno E, Tohno E, Soeda S, et al. Dynamic tests in real-time breast echography. Ultrasound Med Biol 1988;14 Suppl 1:53-57
10. Krouskop TA, Dougherty DR, Vinson FS. A pulsed Doppler ultrasonic system for making noninvasive measurements of the mechanical properties of soft tissue. J Rehabil Res Dev 1987;24:1-8
11. Ophir J, Cespedes I, Ponnekanti H, Yazdi Y, Li X. Elastography: a quantitative method for imaging the elasticity of biological tissues. Ultrason Imaging 1991;13:111-134
12. Ophir J. http://www.uth.tmc.edu/schools/med/rad/elasto/
13. Parker KJ, Doyley MM, Rubens DJ. Imaging the elastic properties of tissue: the 20 year perspective. Phys Med Biol 2011;56:R1-R29
14. Gregersen H, Matre K. The Use of Ultrasound in Biomechanics. In: Ødegaard S, Gilja OH, Gregersen H eds, Basic and New Aspects of Gastrointestinal Ultrasonography. Singapore: World scientific Publishing Co. Pte. Ltd; 2005:23-53
15. Krouskop TA, Wheeler TM, Kallel F, Garra BS, Hall T. Elastic moduli of breast and prostate tissues under compression. Ultrason Imaging 1998;20:260-274
16. Shiina T DM, Bamber JC. Strain imaging using combined RF and envelope autocorrelation processing. In, Ultrasonics Symposium, 1996 IEEE Proceedings; 1996:1331-1336
17. Shiina T YM. Fast reconstruction of tissue elastic modulus image by ultrasound. In, Engineering in Medicine and Biology 2005. Shanghai, China: Proceedings of 2005 IEEE; 2005:976-980
18. Salcudean SE, French D, Bachmann S, et al. Viscoelasticity modeling of the prostate region using vibro-elastography. Med Image Comput Comput Assist Interv 2006;9:389-396
19. Fatemi M, Greenleaf JF. Probing the dynamics of tissue at low frequencies with the radiation force of ultrasound. Phys Med Biol 2000;45:1449-1464
20. Alizad A, Whaley DH, Greenleaf JF, Fatemi M. Image features in medical vibro-acoustography: in vitro and in vivo results. Ultrasonics 2008;48:559-562

21. Urban MW, Chalek C, Kinnick RR, et al. Implementation of vibro-acoustography on a clinical ultrasound system. IEEE Trans Ultrason Ferroelectr Freq Control 2011;58:1169-1181
22. Deffieux T, Montaldo G, Tanter M, Fink M. Shear wave spectroscopy for in vivo quantification of human soft tissues visco-elasticity. IEEE Trans Med Imaging 2009;28:313-322
23. Palmeri ML, Nightingale KR. Acoustic radiation force-based elasticity imaging methods. Interface Focus 2011;1:553-564
24. Lai WM, Rubin D, Krempl E. Introduction to continuum mechanics. Woburn, MA: Butterworth-Heinmann; 1999
25. Palmeri ML, Frinkley KD, Zhai L, et al. Acoustic radiation force impulse (ARFI) imaging of the gastrointestinal tract. Ultrason Imaging 2005;27:75-88
26. Palmeri ML, Wang MH, Rouze NC, et al. Noninvasive evaluation of hepatic fibrosis using acoustic radiation force-based shear stiffness in patients with nonalcoholic fatty liver disease. J Hepatol 2011;55:666-672
27. Castera L, Vergniol J, Foucher J, et al. Prospective comparison of transient elastography, Fibrotest, APRI, and liver biopsy for the assessment of fibrosis in chronic hepatitis C. Gastroenterology 2005;128:343-350
28. Fraquelli M, Rigamonti C, Casazza G, et al. Reproducibility of transient elastography in the evaluation of liver fibrosis in patients with chronic liver disease. Gut 2007;56:968-973
29. Rockey DC. Noninvasive assessment of liver fibrosis and portal hypertension with transient elastography. Gastroenterology 2008;134:8-14
30. Bavu E, Gennisson JL, Couade M, et al. Noninvasive in vivo liver fibrosis evaluation using supersonic shear imaging: a clinical study on 113 hepatitis C virus patients. Ultrasound Med Biol 2011;37:1361-1373
31. Muller M, Gennisson JL, Deffieux T, Tanter M, Fink M. Quantitative viscoelasticity mapping of human liver using supersonic shear imaging: preliminary in vivo feasibility study. Ultrasound Med Biol 2009;35:219-229
32. Foucher J, Chanteloup E, Vergniol J, et al. Diagnosis of cirrhosis by transient elastography (FibroScan): a prospective study. Gut 2006;55:403-408
33. Sandrin L, Tanter M, Gennisson JL, Catheline S, Fink M. Shear elasticity probe for soft tissues with 1-D transient elastography. IEEE Trans Ultrason Ferroelectr Freq Control 2002;49:436-446
34. Tanter M, Bercoff J, Sandrin L, Fink M. Ultrafast compound imaging for 2-D motion vector estimation: application to transient elastography. IEEE Trans Ultrason Ferroelectr Freq Control 2002;49:1363-1374
35. Friedrich-Rust M, Ong MF, Martens S, et al. Performance of transient elastography for the staging of liver fibrosis: a meta-analysis. Gastroenterology 2008;134:960-974
36. Sporea I, Sirli R, Deleanu A, Popescu A, Cornianu M. Liver stiffness measurement by transient elastography in clinical practice. J Gastrointestin Liver Dis 2008;17:395-399
37. Nightingale K, Palmeri M, Trahey G. Analysis of contrast in images generated with transient acoustic radiation force. Ultrasound Med Biol 2006;32:61-72
38. D'Onofrio M, Gallotti A, Mucelli R. Tissue quantification with acoustic radiation force impulse imaging: Measurement repeatability and normal values in the healthy liver. Am J Roentgenol 2010;1:132-136
39. Gallotti A, D'Onofrio M, Pozzi Mucelli R. Acoustic Radiation Force Impulse (ARFI) technique in ultrasound with Virtual Touch tissue quantification of the upper abdomen. Radiol Med 2010;115:889-897

40. McAleavey S, Collins E, Kelly J, Elegbe E, Menon M. Validation of SMURF estimation of shear modulus in hydrogels. Ultrason Imaging 2009;31:131-150
41. McAleavey S, Menon M, Elegbe E. Shear modulus imaging with spatially-modulated ultrasound radiation force. Ultrason Imaging 2009;31:217-234
42. Bercoff J, Pernot M, Tanter M, Fink M. Monitoring thermally-induced lesions with supersonic shear imaging. Ultrason Imaging 2004;26:71-84
43. Bercoff J, Tanter M, Fink M. Supersonic shear imaging: a new technique for soft tissue elasticity mapping. IEEE Trans Ultrason Ferroelectr Freq Control 2004;51:396-409
44. Gennisson JL, Muller M, Deffieux T, Tanter M, Fink M. Quantitative Viscoelasticity Mapping of Human Liver Using Supersonic Shear Imaging: Preliminary in Vivo Feasability Study. Ultrasound in Medicine and Biology 2009;35:219-229
45. Tanter M, Bercoff J, Athanasiou A, et al. Quantitative assessment of breast lesion viscoelasticity: initial clinical results using supersonic shear imaging. Ultrasound Med Biol 2008;34:1373-1386
46. Heimdal A, Gilja OH. Strain Rate Imaging - A new tool for studying the GI tract. In: Odegaard S, Gilja OH, Gregersen H ed, Basic and new aspects of gastrointestinal ultrasonography. Singapore: World Scientific; 2005:243-263
47. Sutherland GR, Stewart MJ, Groundstroem KW, et al. Color Doppler myocardial imaging: a new technique for the assessment of myocardial function. J Am Soc Echocardiogr 1994;7:441-458
48. Castro PL, Greenberg NL, Drinko J, Garcia MJ, Thomas JD. Potential pitfalls of strain rate imaging: angle dependency. Biomed Sci Instrum 2000;36:197-202
49. Thorstensen A, Amundsen BH, Dalen H, et al. Strain rate imaging combined with wall motion analysis gives incremental value in direct quantification of myocardial infarct size. Eur Heart J Cardiovasc Imaging 2012
50. Oxborough D, George K, Birch KM. Intraobserver Reliability of Two-Dimensional Ultrasound Derived Strain Imaging in the Assessment of the Left Ventricle, Right Ventricle, and Left Atrium of Healthy Human Hearts. Echocardiography 2012
51. Ahmed AB, Gilja OH, Hausken T, Gregersen H, Matre K. Strain measurement during antral contractions by ultrasound strain rate imaging: influence of erythromycin. Neurogastroenterol Motil 2009;21:170-179
52. Gilja OH, Heimdal A, Hausken T, et al. Strain during gastric contractions can be measured using Doppler ultrasonography. Ultrasound Med Biol 2002;28:1457-1465
53. Ahmed AB, Gilja OH, Gregersen H, Odegaard S, Matre K. In vitro strain measurement in the porcine antrum using ultrasound doppler strain rate imaging. Ultrasound Med Biol 2006;32:513-522
54. Madsen EL, Frank GR, Krouskop TA, et al. Tissue-mimicking oil-in-gelatin dispersions for use in heterogeneous elastography phantoms. Ultrason Imaging 2003;25:17-38
55. Fromageau J, Gennisson JL, Schmitt C, et al. Estimation of polyvinyl alcohol cryogel mechanical properties with four ultrasound elastography methods and comparison with gold standard testings. IEEE Trans Ultrason Ferroelectr Freq Control 2007;54:498-509
56. Pavan TZ, Madsen EL, Frank GR, Adilton OCA, Hall TJ. Nonlinear elastic behavior of phantom materials for elastography. Phys Med Biol 2010;55:2679-2692
57. Browne JE, Ramnarine KV, Watson AJ, Hoskins PR. Assessment of the acoustic properties of common tissue-mimicking test phantoms. Ultrasound Med Biol 2003;29:1053-1060

58. Larsen IK, Grimsrud TK, Haldorsen T, et al. Cancer in Norway 2009. Oslo: Norwegian Cancer Registry; 2011
59. Moum B, Vatn MH, Ekbom A, et al. Incidence of Crohn's disease in four counties in southeastern Norway, 1990-93. A prospective population-based study. The Inflammatory Bowel South-Eastern Norway (IBSEN) Study Group of Gastroenterologists. Scand J Gastroenterol 1996;31:355-361
60. Fonager K, Sorensen HT, Olsen J. Change in incidence of Crohn's disease and ulcerative colitis in Denmark. A study based on the National Registry of Patients, 1981-1992. Int J Epidemiol 1997;26:1003-1008
61. Loftus EV, Jr., Silverstein MD, Sandborn WJ, et al. Crohn's disease in Olmsted County, Minnesota, 1940-1993: incidence, prevalence, and survival. Gastroenterology 1998;114:1161-1168
62. van Heerde MJ, Biermann K, Zondervan PE, et al. Prevalence of Autoimmune Pancreatitis and Other Benign Disorders in Pancreatoduodenectomy for Presumed Malignancy of the Pancreatic Head. Dig Dis Sci 2012
63. Odegaard S, Nesje LB, Ohm IM, Kimmey MB. Endosonography in gastrointestinal diseases. Acta Radiol 1999;40:119-134
64. Odegaard S, Nesje LB, Lærum OD, Kimmey MB. High-frequency ultrasonographic imaging of the gastrointestinal wall. Expert Review of Medical Devices 2012;9:263-273
65. Odegaard S, Nesje LB, Gilja OH. Atlas of Endoscopic Ultrasonography. Bergen: Fagbokforlaget; 2007
66. Nesje LB, Odegaard S, Kimmey MB. Transendoscopic ultrasonography during conventional upper gastrointestinal endoscopy. Clinical evaluation of a linear 20-MHz probe system. Scand J Gastroenterol 1997;32:500-508
67. Chen TH, Lin CJ, Wu RC, et al. The application of miniprobe ultrasonography in the diagnosis of colorectal subepithelial lesions. Chang Gung Med J 2010;33:380-388
68. May A, Gunter E, Roth F, et al. Accuracy of staging in early oesophageal cancer using high resolution endoscopy and high resolution endosonography: a comparative, prospective, and blinded trial. Gut 2004;53:634-640
69. Nesje LB, Svanes K, Viste A, Laerum OD, Odegaard S. Comparison of a linear miniature ultrasound probe and a radial-scanning echoendoscope in TN staging of esophageal cancer. Scand J Gastroenterol 2000;35:997-1002
70. Dumonceau JM, Polkowski M, Larghi A, et al. Indications, results, and clinical impact of endoscopic ultrasound (EUS)-guided sampling in gastroenterology: European Society of Gastrointestinal Endoscopy (ESGE) Clinical Guideline. Endoscopy 2011;43:897-912
71. Vilmann P, Saftoiu A. Endoscopic ultrasound-guided fine needle aspiration biopsy: equipment and technique. J Gastroenterol Hepatol 2006;21:1646-1655
72. Hassan H, Vilmann P, Sharma V. Impact of EUS-guided FNA on management of gastric carcinoma. Gastrointest Endosc 2010;71:500-504
73. Hasan MK, Hawes RH. EUS-Guided FNA of Solid Pancreas Tumors. Gastrointest Endosc Clin N Am 2012;22:155-167
74. Itoh A, Ueno E, Tohno E, et al. Breast disease: clinical application of US elastography for diagnosis. Radiology 2006;239:341-350
75. Giovannini M, Hookey LC, Bories E, et al. Endoscopic ultrasound elastography: the first step towards virtual biopsy? Preliminary results in 49 patients. Endoscopy 2006;38:344-348

76. Janssen J, Schlorer E, Greiner L. EUS elastography of the pancreas: feasibility and pattern description of the normal pancreas, chronic pancreatitis, and focal pancreatic lesions. Gastrointest Endosc 2007;65:971-978
77. Soleimanpour H, Hassanzadeh K, Vaezi H, et al. Effectiveness of intravenous lidocaine versus intravenous morphine for patients with renal colic in the emergency department. BMC Urol 2012;12:13
78. Phan NQ, Blome C, Fritz F, et al. Assessment of Pruritus Intensity: Prospective Study on Validity and Reliability of the Visual Analogue Scale, Numerical Rating Scale and Verbal Rating Scale in 471 Patients with Chronic Pruritus. Acta Derm Venereol 2011
79. Hendey GW, Donner NF, Fuller K. Clinically significant changes in nausea as measured on a visual analog scale. Ann Emerg Med 2005;45:77-81
80. Haldorsen K, Bjelland I, Bolstad AI, Jonsson R, Brun JG. A five-year prospective study of fatigue in primary Sjogren's syndrome. Arthritis Res Ther 2011;13:R167
81. Grant S, Aitchison T, Henderson E, et al. A comparison of the reproducibility and the sensitivity to change of visual analogue scales, Borg scales, and Likert scales in normal subjects during submaximal exercise. Chest 1999;116:1208-1217
82. Havre RF, Waage JR, Gilja OH, Odegaard S, Nesje LB. Real-Time Elastography: Strain Ratio Measurements Are Influenced by the Position of the Reference Area. Ultraschall in Med 2011. E-pub ahead of print June 2011.
83. Landis JR, Koch GG. The measurement of observer agreement for categorical data. Biometrics 1977;33:159-174
84. Bland JM, Altman DG. Statistical methods for assessing agreement between two methods of clinical measurement. Lancet 1986;1:307-310
85. Zeger SL, Liang KY. Longitudinal data analysis for discrete and continuous outcomes. Biometrics 1986;42:121-130
86. de Araujo VC, Furuse C, Cury PR, et al. Desmoplasia in different degrees of invasion of carcinoma ex-pleomorphic adenoma. Head Neck Pathol 2007;1:112-117
87. Ohtani H. Pathophysiologic significance of host reactions in human cancer tissue: desmoplasia and tumor immunity. Tohoku J Exp Med 1999;187:193-202
88. Deak SB, Glaug MR, Pierce RA, et al. Desmoplasia in benign and malignant breast disease is characterized by alterations in level of mRNAs coding for types I and III procollagen. Matrix 1991;11:252-258
89. Crnogorac-Jurcevic T, Efthimiou E, Capelli P, et al. Gene expression profiles of pancreatic cancer and stromal desmoplasia. Oncogene 2001;20:7437-7446
90. Lohr M, Schmidt C, Ringel J, et al. Transforming growth factor-beta1 induces desmoplasia in an experimental model of human pancreatic carcinoma. Cancer Res 2001;61:550-555
91. Pandol S, Edderkaoui M, Gukovsky I, Lugea A, Gukovskaya A. Desmoplasia of pancreatic ductal adenocarcinoma. Clin Gastroenterol Hepatol 2009;7:S44-47
92. Lunt SJ, Kalliomaki TM, Brown A, et al. Interstitial fluid pressure, vascularity and metastasis in ectopic, orthotopic and spontaneous tumours. BMC Cancer 2008;8:2
93. Wiig H, Noddeland H. Interstitial fluid pressure in human skin measured by micropuncture and wick-in-needle. Scand J Clin Lab Invest 1983;43:255-260
94. Wiig H, Tveit E, Hultborn R, Reed RK, Weiss L. Interstitial fluid pressure in DMBA-induced rat mammary tumours. Scand J Clin Lab Invest 1982;42:159-164
95. Heldin CH, Rubin K, Pietras K, Ostman A. High interstitial fluid pressure - an obstacle in cancer therapy. Nat Rev Cancer 2004;4:806-813

96. Milosevic MF, Fyles AW, Hill RP. The relationship between elevated interstitial fluid pressure and blood flow in tumors: a bioengineering analysis. Int J Radiat Oncol Biol Phys 1999;43:1111-1123
97. Mateen MA, Muheet KA, Mohan RJ, et al. Evaluation of ultrasound based acoustic radiation force impulse (ARFI) and eSie touch sonoelastography for diagnosis of inflammatory pancreatic diseases. JOP 2012;13:36-44
98. Barr RG, Memo R, Schaub CR. Shear wave ultrasound elastography of the prostate: initial results. Ultrasound Q 2012;28:13-20
99. Barbone PE, Bamber JC. Quantitative elasticity imaging: what can and cannot be inferred from strain images. Phys Med Biol 2002;47:2147-2164
100. Hofmann M, McCormack E, Mujic M, et al. Increased plasma colloid osmotic pressure facilitates the uptake of therapeutic macromolecules in a xenograft tumor model. Neoplasia 2009;11:812-822
101. Waage JE, Havre RF, Odegaard S, et al. Endorectal elastography in the evaluation of rectal tumours. Colorectal Dis 2011;13:1130-1137
102. Iglesias-Garcia J, Larino-Noia J, Abdulkader I, Forteza J, Dominguez-Munoz JE. Quantitative endoscopic ultrasound elastography: an accurate method for the differentiation of solid pancreatic masses. Gastroenterology 2010;139:1172-1180
103. Itokawa F, Itoi T, Sofuni A, et al. EUS elastography combined with the strain ratio of tissue elasticity for diagnosis of solid pancreatic masses. J Gastroenterol 2011;46:843-853
104. Saftoiu A, Vilmann P, Gorunescu F, et al. Neural network analysis of dynamic sequences of EUS elastography used for the differential diagnosis of chronic pancreatitis and pancreatic cancer. Gastrointest Endosc 2008;68:1086-1094
105. Hirche TO, Ignee A, Barreiros AP, et al. Indications and limitations of endoscopic ultrasound elastography for evaluation of focal pancreatic lesions. Endoscopy 2008;40:910-917
106. Giovannini M, Thomas B, Erwan B, et al. Endoscopic ultrasound elastography for evaluation of lymph nodes and pancreatic masses: a multicenter study. World J Gastroenterol 2009;15:1587-1593
107. Iglesias-Garcia J, Larino Noia J, Alvarez Castro A, Cigarran B, Dominguez Munoz JE. Second-generation endoscopic ultrasound elastography in the differential diagnosis of solid pancreatic masses. Pancreatic cancer vs. inflammatory mass in chronic pancreatitis. Rev Esp Enferm Dig 2009;101:723-730
108. Saftoiu A, Vilmann P, Gorunescu F, et al. Accuracy of endoscopic ultrasound elastography used for differential diagnosis of focal pancreatic masses: a multicenter study. Endoscopy 2011;43:596-603
109. Saftoiu A, Vilmann P, Gorunescu F, et al. Efficacy of an artificial neural network-based approach to endoscopic ultrasound elastography in diagnosis of focal pancreatic masses. Clin Gastroenterol Hepatol 2012;10:84-90
110. Franquet A, Avril S, Le Riche R, Badel P. Identification of heterogeneous elastic properties in stenosed arteries: a numerical plane strain study. Comput Methods Biomech Biomed Engin 2012;15:49-58
111. Rosario DE, Brigham JC, Aquino W. Identification of material properties of orthotropic elastic cylinders immersed in fluid using vibroacoustic techniques. Ultrasonics 2008;48:547-552